AIAA JOURNAL
Vol. 45, No. 7, July 2007

Lattice Boltzmann Method Simulation of Aeroacoustics and Nonreflecting Boundary Conditions

E. W. S. Kam,* R. M. C. So,† and R. C. K. Leung‡
Hong Kong Polytechnic University, Hong Kong, People's Republic of China

DOI: 10.2514/1.27632

A lattice Boltzmann method that can recover the first coefficient of viscosity and the specific heat ratio correctly has been adopted for one-step aeroacoustic simulations because it can recover the speed of sound correctly. Instead of solving the Navier–Stokes equations as in the case of direct numerical simulation, the lattice Boltzmann method only needs to solve one transport equation for the collision function. Other flow properties are obtained by integrating this collision function over the particle velocity space. The lattice Boltzmann method is effective only if appropriate nonreflecting boundary conditions for open computational boundaries are available, just like the direct numerical simulation. Four different nonreflecting boundary conditions are commonly used with direct numerical simulation for one-step aeroacoustic simulations. Among these are the characteristics-based method, the perfectly matched layer method, the C^1 continuous method, and the absorbing layer method. Not all nonreflecting boundary conditions are applicable when used with the lattice Boltzmann method; some might not be appropriate, whereas others could be rather effective. This paper examines some existing nonreflecting boundary conditions plus other new proposals, their appropriateness, and their suitability for the lattice Boltzmann method. The assessment is made against two classic aeroacoustic problems: propagation of a plane pressure pulse and propagation of acoustic, entropy, and vortex pulses in a uniform stream. A reference solution is obtained using direct numerical simulation assuming a relatively large computational domain without any specified nonreflecting boundary conditions. The results, obtained with a computational domain half the size of that used for the direct numerical simulation calculations, show that the absorbing layer method and the extrapolation method with assumed filter perform the best.

Nomenclature

b	=	arbitrary variable
c	=	sound speed
c_∞	=	reference sound speed
D	=	width of damping region
D_n	=	dimension number
e	=	internal energy of fluid
$f(\boldsymbol{x}, \boldsymbol{\xi}, t)$	=	particle distribution function
f_a	=	prescribed f at outlet boundary of the absorbing region
f^{eq}	=	equilibrium state of f
L	=	characteristic length scale
$\|L_p(b)\|$	=	error integral of b
$\|L_\infty(b)\|$	=	maximum of error given by $\max_j \lvert b_{\text{LBM},j} - b_{\text{DNS},j}\rvert$
p	=	pressure
R	=	universal gas constant
T	=	fluid temperature
t	=	time
U	=	characteristic velocity scale
$\boldsymbol{u}\,(u, v)$	=	fluid velocity vector
u	=	x-direction velocity
v	=	y-direction velocity
$\boldsymbol{x}\,(x, y)$	=	spatial vector
x	=	stream coordinate
y	=	normal coordinate
γ	=	specific heat ratio
Δt	=	time step
Δx	=	grid length along x
Δy	=	grid length along y
δ	=	distance measured from start of damping region
κ	=	thermal conductivity
μ	=	first coefficient of viscosity
$\boldsymbol{\xi}$	=	microscopic particle velocity vector
ρ	=	fluid density
ρ_∞	=	reference fluid density
σ	=	absorption coefficient
τ	=	collision relaxation time
τ_{eff}	=	effective collision relaxation time
τ_1	=	translational relaxation time
τ_2	=	rotational relaxation time

Subscripts

i, j	=	indices for grid or velocity lattice
∞	=	denotes upstream condition

Presented as Paper 2416 at the 12th AIAA/CEAS Aeroacoustics Conference (27th AIAA Aeroacoustics Conference), Cambridge, MA, 8–10 May 2006; received 4 September 2006; revision received 15 February 2007; accepted for publication 15 February 2007.

*Ph.D. Student, Department of Mechanical Engineering, Hung Hom, Kowloon.

†Emeritus Professor, Department of Mechanical Engineering, Hung Hom, Kowloon, also the Industrial Center; mmmcso@polyu.edu.hk (corresponding author).

‡Assistant Professor, Department of Mechanical Engineering, Hung Hom, Kowloon.

I. Introduction

THE numerical methods used to carry out direct aeroacoustic simulations have to be capable of resolving the disparity in scales between the aerodynamic and acoustic disturbances. However, they are not the only vital component that is important for an accurate resolution of the problem. Most aeroacoustic simulation problems are concerned with open boundaries. All numerical simulations have to invoke truncated boundaries because current computer capacity cannot accommodate infinite boundaries; it is most crucial that all truncated boundaries would not only allow the aerodynamic disturbances but also the acoustic waves to pass through with no reflection. Otherwise, the reflected acoustic waves would interact with the forward-going waves to produce disturbances that could be of the same order as the acoustic waves themselves. The errors thus created cannot be distinguished from the

true acoustic waves and the direct aeroacoustic simulation is not reliable. Therefore, a discussion of direct aeroacoustic simulation has to address the numerical method employed as well as the nonreflecting boundary conditions (NRBC) to be invoked for the truncated open boundaries. These two components are briefly discussed in the following paragraphs.

Up to now, one-step aeroacoustic simulations have been carried out by solving the mass, momentum and energy conservation equation, and the gas equation of state. Because the acoustic field has very low-energy contents, a low dispersive and low dissipative scheme is required if wave propagation were to be resolved accurately in a direct aeroacoustic simulation. A direct numerical simulation (DNS) scheme that satisfies these requirements has been proposed [1] and it is made up of a sixth-order compact finite-difference scheme and a fourth-order Runge–Kutta time-marching technique. The scheme was later improved [2,3] and the improved version has been used to study aeroacoustic problems and was found to be able to resolve the acoustic field with velocity fluctuations five orders of magnitude smaller than any mean field fluctuations [4].

The DNS scheme is numerically rather complicated. Efforts to simplify the numeric led to the exploration of an alternate numerical scheme based on the Boltzmann equation (BE) [5–7]. Typically, the BE is solved using a lattice Boltzmann method (LBM). The LBM is simple because it only needs to solve one transport equation for the particle distribution function $f(\boldsymbol{x}, \boldsymbol{\xi}, t)$, rather than a mixed set of tensor, vector, and scalar equations as in the case of DNS. The flow properties are obtained by integrating f over the particle velocity space. Its simplicity attracts researchers to extend the LBM to carry out one-step aeroacoustic simulationns [8–11]. Other proposals, based on the lattice kinetic equation [12] and the direct simulation Monte Carlo [13], have also been put forward. In these methods and the LBM, it is not clear whether the speed of sound c has been recovered correctly because they follow the practice of DNS by specifying the Mach number M as an input to the problem. However, this is not necessary for a gas kinetic approach because, in principle, once f is obtained from the BE, the thermodynamic properties of the gas can be determined and hence c and M. Therefore, it is important to recover the gas equation of state correctly; that is, the specific heat ratio $\gamma = 1.4$ for air for aeroacoustic simulation. One of the reasons for this deficiency could be due to the fact that, inherent in the original LBM proposal [7], the compressible form of the Navier–Stokes equations could be recovered but not the correct transport coefficients and proper gas equation of state [9,10,14]. This means that the theoretical relation between c and the internal energy e of the fluid cannot be replicated. As a result, it is not sure whether M can be determined correctly over the whole flowfield.

Two improvements are required before current LBM can be extended with confidence to simulate aeroacoustics. First, it is necessary to modify the modeled BE so that it can fully recover the complete set of compressible Navier–Stokes equations, that is, the mass, momentum and energy conservation equations with the correct transport coefficients, and the gas equation of state (at least for a diatomic gas). Second, it is necessary to formulate appropriate NRBC for use with the improved LBM. This latter improvement is the objective of the present study.

For a truncated computational domain, precise boundary conditions play a key role in aeroacoustic calculation. At some boundaries, such as the inflow and outflow boundaries, the assumed computational boundaries have to allow the aerodynamic field to pass freely with minimal reflection while at the same time they should be nonreflecting for the incident acoustic waves. Otherwise, the spurious erroneous waves reflecting from the boundaries could contaminate the numerical simulations, decrease the computational accuracy, and might even drive the solutions towards a wrong time-stationary state. These requirements are particularly important in one-step numerical simulation of aeroacoustics of open flows, because reflecting waves at open boundaries are strictly prohibited. Otherwise, the acoustic radiation condition will be violated. Therefore, the implementation of NRBC at the computational boundaries is not only necessary but required in the simulation of aeroacoustic problems.

There have been numerous attempts to develop truly NRBC for one-step aeroacoustic simulation using DNS. The classical 1-D nonreflecting characteristics-based boundary condition (NSCBC) is the most widely used because of its simplicity. Different NSCBC schemes have been proposed [15–19]. Another NRBC is the absorbing boundary conditions (ABC) [20–22]. A convective term was added to the linear Euler equations, thereby forcing the solution to become supersonic at the border of the computational domain [21]. An alternative proposal was to recast the Navier–Stokes equations with additional damping terms so that all flow unsteadiness were suppressed and the flow was forced towards a prescribed uniform flow in a buffer zone beyond the physical domain [22]. This proposal has one drawback though, because it requires an a priori knowledge of the outlet flow. Other not as commonly used boundary treatment methods include the filtering method (FM) applied to the whole spatial field [2,3], the perfectly matched layer (PML) method [23], and the C^1 continuity preservation method [24,25]. All these methods are successful for some types of problems and are less so for others.

As is the case in DNS simulations, NRBC for open boundaries have to be formulated for LBM. All the boundary treatment schemes mentioned in the preceding paragraphs have been applied to DNS calculations only; few have been extended to LBM. Instead, extrapolation method (EM) is applied to the zeroth or first order of f. In the study of Tsutahara et al. [9], a prescribed boundary condition is specified for the density, but no details on implementation have been given. On the other hand, Kang et al. [10] stipulates a NSCBC boundary conditions along the line of Poinsot and Lele [17]. Again, no details are provided on how to implement the NSCBC.

The improved LBM [26,27] with zero f gradients (ZFG) assumed at open boundaries was used to simulate three benchmark aeroacoustic problems. Its computational accuracy was established by comparing the results of the three benchmark simulations with those obtained from DNS. In the DNS calculations, the errors arising from reflection at the boundaries were minimized by adopting a relatively large domain with damping region in the simulation. The results show that the LBM calculations [26,27] with a smaller domain are just as accurate as those obtained using DNS with a larger computational domain. However, the study did not examine the merits of other types of NRBC; therefore, the relative merits and accuracy of the respective boundary treatments on LBM aeroacoustic simulations need further investigation.

II. Lattice Boltzmann Method

To assess the effectiveness of the different NRBC for aeroacoustic simulations using LBM, an LBM that can simulate the fluid properties correctly is required. Such an LBM has been derived by Li et al. [26]. For the sake of completeness, the inadequacy of the conventional LBM is first pointed out and this is followed by a summary of the remedies made to correctly recover the fluid properties [26]. This improved LBM is used in the present study.

A. Conventional LBM

The governing equation of the LBM is the BE modeled by adopting the Bhatnagar, Gross, and Krook (BGK) [28] collision model. In this equation, the particle distribution function f has the dimensions of $(\mathrm{m/s})^{-3} \cdot \mathrm{m}^{-3}$. The dimensionless form of the modeled equation is given by

$$\frac{\partial f}{\partial t} + \boldsymbol{\xi} \cdot \nabla f = -\frac{1}{\tau}(f - f^{\mathrm{eq}}) \tag{1}$$

where τ is the time taken for f to relax from nonequilibrium to an equilibrium state f^{eq}. All variables in the dimensional BE have been normalized by using a combination of the reference parameters, ρ_∞, c_∞, and L. Usually, the dense gas assumption was invoked to make use of the Chapman–Enskog expansion to derive the complete set of compressible Navier–Stokes equations and their transport coefficients from the BGK-modeled BE [7]. Only the translational degree of freedom was considered in formulating the BGK model; as

a result, the particles were assumed to undergo rigid collision with a relaxation time τ. This assumption led to $\gamma = (D_n + 2)/D_n$, $\mu = \rho RT\tau$, and $\kappa = c_p\mu$, where c_p is specific heat at constant pressure. Therefore, 3-D flow of monoatomic gases gives $\gamma = 1.67$ and 2-D flow yields $\gamma = 2$. The conventional LBM solving the BGK-modeled BE was unable to replicate the full set of compressible Navier–Stokes equations with correct transport coefficients and γ, and was not appropriate for aeroacoustic simulations. Therefore, further improvements are required if γ and the transport coefficients were to be recovered correctly.

B. Improved LBM

The improved LBM [26] attempts to accomplish this by following a two-step approach. The first step concentrates on the recovery of γ and μ, whereas the second step focuses on deriving κ correctly. It should be pointed out that in the present formulation, μ and κ are the dimensionless counterparts of the fluid viscosity and thermal conductivity; they are normalized by $\rho_\infty cL$. Effort to accomplish the first step has been made by including both the translational and rotational degree of freedom into the derivation of an effective relaxation time τ_{eff} to replace τ in Eq. (1). This τ_{eff} was assumed to be made up of two relaxation times, τ_1 and τ_2. It was found that τ_1 is essentially given by the rigid-sphere collision model, that is, τ, and τ_2 can be determined exactly with no arbitrary constant by stipulating that the derived μ should obey the Sutherland law. This improvement, however, could not rectify the error in the prediction of κ, which, according to this formulation, is given by $\kappa = c_p\mu$, thus leading to a Prandtl number $Pr = c_p\mu/\kappa = 1$ for diatomic gases.

It is anticipated that κ could be recovered correctly by invoking Eucken's model for the derivation of the macroscopic heat flux with perhaps a third relaxation time. However, this third relaxation time could be shown to relate to τ_{eff}. Thus derived, the Fourier law of heat conduction can also be recovered. This second step is currently being pursued. It is anticipated that with the completion of this second step, the improved LBM will be able to replicate μ, γ, and κ correctly, thus leading to a correct estimate of the Reynolds number, $Re = \rho UL/\mu^*$, the Mach number $M = U/c$, and Pr, in a low-Reynolds-number, shock-free compressible flow. Here, μ^* is the dimensional μ.

III. Numerical Solution of the Improved LBM

The modeled Eq. (1) is solved numerically by first discretizing it in a velocity space using a finite set of velocity vectors $\{\boldsymbol{\xi}_i\}$ in the context of the conservation laws. Here, the subscript i is only an index and is not a vector or tensor notation. A local Maxwellian is used to represent f^{eq} and a Taylor expansion up to third order in $\boldsymbol{u}$ is assumed. This can be expressed in the discrete velocity space as

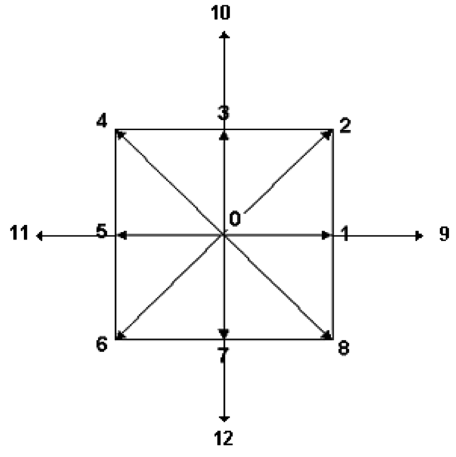

Fig. 1 Definition of the D2Q13 lattice velocity model.

$$f^{\text{eq}} = \rho A_i\left\{1 + \frac{\boldsymbol{\xi}\cdot\boldsymbol{u}}{\theta} + \frac{1}{2}\left(\frac{\boldsymbol{\xi}\cdot\boldsymbol{u}}{\theta}\right)^2 - \frac{\boldsymbol{u}^2}{2\theta} - \frac{(\boldsymbol{\xi}\cdot\boldsymbol{u})\boldsymbol{u}^2}{2\theta^2} + \mathcal{O}\left(\frac{(\boldsymbol{\xi}\cdot\boldsymbol{u})^3}{\theta^3}\right)\right\} \tag{2}$$

where $\boldsymbol{u} = (u, v)$ and $\theta = RT/c^2$. The weighting factors A_i are dependent on the lattice model selected to represent the discrete velocity space. They are evaluated from the constraints of the local macroscopic variables, such as ρ, momentum $\rho\boldsymbol{u}$, internal energy e, and pressure p, given by the integrals of f and $\boldsymbol{\xi}$ over the velocity space in the lattice with N discrete velocity sets $\{\boldsymbol{\xi}_i\}$.

A discrete velocity set given by a D2Q13 (2-D with 13 velocity points) lattice model is adopted here, because D2Q13 has been shown to give very reliable and accurate results by Li et al. [26,27]. The velocity lattice is shown in Fig. 1, and the discrete velocity set and weighting factors A_i are given by

$$\begin{aligned}
&\boldsymbol{\xi}_i = 0\\
&\boldsymbol{\xi}_i = \left\{\cos\left(\frac{\pi(i-1)}{4}\right), \sin\left(\frac{\pi(i-1)}{4}\right)\right\}, \qquad i = 1, 3, 5, 7\\
&\boldsymbol{\xi}_i = \sqrt{2}\left\{\cos\left(\frac{\pi(i-1)}{4}\right), \sin\left(\frac{\pi(i-1)}{4}\right)\right\}, \qquad i = 2, 4, 6, 8\\
&\boldsymbol{\xi}_i = 2\left\{\cos\left(\frac{\pi(i-1)}{4}\right), \sin\left(\frac{\pi(i-1)}{4}\right)\right\}, \qquad i = 9, 10, 11, 12
\end{aligned} \tag{3a}$$

$$\begin{aligned}
A_0 &= 1 - \frac{5}{2}\theta + \left(-\frac{3}{2} + 2\gamma\right)\theta^2\\
A_1 = A_3 = A_5 = A_7 &= \frac{2}{3}\theta + (1-\gamma)\theta^2\\
A_2 = A_4 = A_6 = A_8 &= \left(-\frac{3}{4} + \frac{1}{2}\gamma\right)\theta^2\\
A_9 = A_{10} = A_{11} = A_{12} &= -\frac{1}{24}\theta + \frac{1}{8}\theta^2
\end{aligned} \tag{3b}$$

The collision term in Eq. (1) is evaluated locally at every time step, whereas a sixth-order compact finite-difference scheme [1] is used to evaluate the nonlinear term and a second-order Runge–Kutta method for time advancement. The lattice size δx is chosen such that $\delta x/\delta t \approx c$, where δt for the lattice motion is chosen to be the same as Δt for time marching and the grid size Δx is taken to be the same as that used in the DNS scheme. This choice of $\delta x/\delta t$ yields very stable numerical solutions for all cases investigated. On boundaries, a one-sided fourth-order compact method is used to derive the first derivatives. This is essentially a low dispersive and low dissipative scheme and is most suitable for simulation of aeroacoustic problems [1–3].

IV. Nonreflecting Boundary Conditions

The commonly used boundary treatment schemes for DNS are NSCBC, PML, ABC, FM, and C^1 continuity, whereas those that have been attempted only for LBM are the EM and ZFG methods. Among the various boundary treatment schemes, some proposed for DNS can be extended to LBM, whereas others cannot. For example, extension of the NSCBC scheme to LBM has been attempted [8] previously. Unfortunately, no details were given on the implementation; therefore, it was difficult to ascertain the general applicability of such an extension. The NSCBC scheme has been carefully examined by Li [29], who chose the propagation in a mean flow of a vortex, entropy, and an acoustic pulse to compare the performance of the NSCBC, PML, and ABC with a reference solution. The simulation was carried out using DNS and the reference solution was obtained using a much larger domain with buffer regions at the inlet and outlet. The results showed that among the

Table 1 Values of a_j, b_j, and $a_{j,i}$

	$j=0$	$j=1$	$j=2$	$j=3$	$j=4$	$j=5$	$j=6$	$j=7$	$j=8$	$j=0$
a_j	$\frac{193+126\alpha}{256}$	$\frac{105+302\alpha}{256}$	$\frac{15(-1+2\alpha)}{64}$	$\frac{45(1-2\alpha)}{512}$	$\frac{5(-1+2\alpha)}{256}$	$\frac{1-2\alpha}{512}$	———	———	———	———
b_j	$\frac{93+70\alpha}{128}$	$\frac{7+18\alpha}{16}$	$\frac{-7+14\alpha}{32}$	$\frac{1-2\alpha}{16}$	$\frac{-1+2\alpha}{128}$	0	———	———	———	———
$a_{j,2}$	———	$\frac{1+254\alpha}{256}$	$\frac{31+2\alpha}{32}$	$\frac{7+50\alpha}{64}$	$\frac{-7+14\alpha}{32}$	$\frac{7(5-10\alpha)}{128}$	$\frac{-7+14\alpha}{32}$	$\frac{7-14\alpha}{64}$	$\frac{-1+2\alpha}{32}$	$\frac{1-2\alpha}{256}$
$a_{j,3}$	———	$\frac{-1+2\alpha}{256}$	$\frac{1+30\alpha}{32}$	$\frac{57+14\alpha}{64}$	$\frac{7+18\alpha}{32}$	$\frac{7(-5+10\alpha)}{128}$	$\frac{7-14\alpha}{32}$	$\frac{-7+14\alpha}{64}$	$\frac{1-2\alpha}{32}$	$\frac{-1+2\alpha}{256}$
$a_{j,4}$	———	$\frac{1-2\alpha}{256}$	$\frac{-1+2\alpha}{32}$	$\frac{7+50\alpha}{64}$	$\frac{25+14\alpha}{32}$	$\frac{35+58\alpha}{128}$	$\frac{-7+14\alpha}{32}$	$\frac{7-14\alpha}{64}$	$\frac{-1+2\alpha}{32}$	$\frac{1-2\alpha}{256}$

schemes tested, PML and ABC gave the least error, whereas NSCBC gave the largest error compared to the reference solution. Straightly speaking, NSCBC works best with normal waves at the boundaries and this was one of the reasons why it performed the worst in this case. It is the objective of this work to seek NRBC that is applicable to all types of waves including normal waves. This shortcoming of the NSCBC together with the assessment of Li [29] renders it inappropriate for extension to LBM simulation.

Applying the C^1 continuity preservation scheme directly to the primitive variables is not a viable alternative for LBM; however, the concept can be extended to LBM. Applying the C^1 continuity preservation scheme concept to LBM implies that the first derivatives of f have to remain continuous across the boundaries, and the inward first derivatives of f will have to be set to zero. This is different from the EM; therefore, it should be tested as an independent method. The PML is not quite applicable for LBM because the LBM only solves a scalar equation for f and the primitive variables are obtained by integrating f over the particle velocity space $\boldsymbol{\xi}$ and an a priori solution is not known for f in any matched layer. However, the concept could be extended by requiring f to approach a target f or f^{eq} at the boundaries. When the PML is implemented this way, it is not much different from the application of ABC to LBM. As will be seen later, applying the ABC to LBM requires the specification of a target f or f^{eq} at the boundaries. In view of this similarity, only the extension of ABC and not the PML to LBM will be considered in this paper. Because the ZFG has been

Table 2 Norm error at $t=9$ for case 1 (compared with DNS solutions): pressure ($\hat{p}=p-p_\infty, \hat{u}=u-u_\infty; \hat{p}_r$ and $\hat{u}_r$ are the reference solutions)

$\|L_P\| = (\frac{1}{n}\sum(\hat{p}-\hat{p}_r)^P)^{\frac{1}{P}}$, $\|L_\infty\| = \max(\hat{p}-\hat{p}_r)$	L_1	L_2	L_∞
EM0	4.2342×10^{-6}	7.5517×10^{-6}	1.9047×10^{-5}
EM0/FM	6.8096×10^{-8}	1.1516×10^{-7}	2.8650×10^{-7}
EM1	4.2377×10^{-6}	7.5587×10^{-6}	1.9064×10^{-5}
EM1/FM	7.2198×10^{-8}	9.4061×10^{-8}	2.1736×10^{-7}
C^1 continuity	1.0677×10^{-6}	1.3857×10^{-6}	3.1877×10^{-6}
ABC	1.8837×10^{-8}	2.0648×10^{-8}	5.4979×10^{-8}

Table 3 Norm error at $t=9$ for case 1 (compared with DNS solutions): velocity ($\hat{p}=p-p_\infty, \hat{u}=u-u_\infty; \hat{p}_r$ and $\hat{u}_r$ are the reference solutions)

$\|L_P\| = (\frac{1}{n}\sum(\hat{u}-\hat{u}_r)^P)^{\frac{1}{P}}$, $\|L_\infty\| = \max(\hat{u}-\hat{u}_r)$	L_1	L_2	L_∞
EM0	4.2409×10^{-6}	7.5617×10^{-6}	1.9096×10^{-5}
EM0/FM	6.2575×10^{-8}	1.0379×10^{-7}	2.7033×10^{-7}
EM1	4.2451×10^{-6}	7.5687×10^{-6}	1.9113×10^{-5}
EM1/FM	6.7929×10^{-8}	1.0123×10^{-7}	2.6062×10^{-7}
C^1 continuity	1.0357×10^{-6}	1.3630×10^{-6}	3.1571×10^{-6}
ABC	2.4918×10^{-8}	3.3341×10^{-8}	8.2538×10^{-8}

Table 4 Norm error at $t=2.6$ for case 2 (compared with DNS solutions): pressure ($\hat{p}=p-p_\infty, \hat{u}=u-u_\infty$; $\hat{p}_r$ and $\hat{u}_r$ are the reference solutions)

$\|L_P\| = (\frac{1}{n}\sum(\hat{p}-\hat{p}_r)^P)^{\frac{1}{P}}$, $\|L_\infty\| = \max(\hat{p}-\hat{p}_r)$	L_1	L_2	L_∞
EM0	5.2606×10^{-5}	7.4286×10^{-5}	3.1617×10^{-4}
EM0/FM	3.1530×10^{-5}	3.6230×10^{-5}	7.5139×10^{-5}
EM1	5.3584×10^{-5}	7.5250×10^{-5}	3.2101×10^{-4}
EM1/FM	5.6519×10^{-5}	6.9461×10^{-5}	1.8350×10^{-4}
C^1 continuity	9.8387×10^{-6}	1.3297×10^{-5}	7.9179×10^{-5}
ABC	2.7005×10^{-6}	3.5453×10^{-6}	1.3460×10^{-5}

Table 5 Norm error at $t=2.6$ for case 2 (compared with DNS solutions): velocity ($\hat{p}=p-p_\infty, \hat{u}=u-u_\infty; \hat{p}_r$ and $\hat{u}_r$ are the reference solutions)

$\|L_P\| = (\frac{1}{n}\sum(\hat{u}-\hat{u}_r)^P)^{\frac{1}{P}}$, $\|L_\infty\| = \max(\hat{u}-\hat{u}_r)$	L_1	L_2	L_∞
EM0	1.8421×10^{-5}	3.2891×10^{-5}	2.0135×10^{-4}
EM0/FM	6.6930×10^{-6}	7.6686×10^{-6}	1.7774×10^{-5}
EM1	1.8483×10^{-5}	3.2924×10^{-5}	2.0126×10^{-4}
EM1/FM	1.1918×10^{-5}	1.4490×10^{-5}	3.8759×10^{-5}
C^1 continuity	1.0370×10^{-5}	2.9847×10^{-5}	1.9847×10^{-4}
ABC	1.5972×10^{-6}	2.1585×10^{-6}	1.0720×10^{-5}

used before to calculate identical benchmark aeroacoustic problems and good agreement with the reference DNS solution is obtained [20], there is no need to repeat the same calculations here again. In fact, the ZFG can be considered a viable nonreflecting boundary treatment scheme for one-step aeroacoustic simulations of the benchmark problems tested [26]. As a result, three types of nonreflecting boundary treatment schemes, namely, 1) EM with or without FM, 2) C^1 continuity, and 3) ABC are tested in the present study. Their suitability for LBM and accuracy are assessed against reference solutions obtained from DNS with a relatively large computational domain. In the DNS calculations, absorbing boundary treatments are applied. The clean solution obtained inside the larger computational domain is used as the reference solution. All error estimates of the LBM calculations are based on this reference. Each type of nonreflecting boundary treatment scheme is briefly described in the following sections.

A. Type 1: EM with or Without FM

This method is fairly easy to implement. Depending on whether zeroth- or first-order extrapolation is assumed, the method simply requires that f or its first gradient in every lattice directions at the computational boundary to be zero [30–34]. It is particularly suitable for LBM because there is only one scalar equation to solve. Of course, a buffer or damping region could be added to improve the performance of the method, but then the scheme would be quite similar to the ABC. Another alternative to improve its performance is to implement the EM with or without a FM. That way, their performance with or without FM could be assessed and compared.

The filtering scheme [2,3] implemented uses a 10th-order low-passed filter. If there are n grid points along the x axis, the equations of a low-passed filtered value $\hat{h}$ for any scalar h can be obtained from

$$i = 1 \quad \text{or} \quad i = n; \qquad \text{no filtering is applied} \tag{4a}$$

$$i \in \{2, 3, 4\} \qquad \alpha\hat{h}_{i-1} + \hat{h} + \alpha\hat{h}_{i+1} = \sum_{j=1}^{9} a_{j,i} h_j \tag{4b}$$

$$i \in \{n-3, n-2, n-1\}$$
$$\alpha\hat{h}_{i-1} + \hat{h} + \alpha\hat{h}_{i+1} = \sum_{j=1}^{9} a_{j,n-i+1} h_{n-j+1} \tag{4c}$$

$$i = 5 \quad \text{or} \quad i = n-4$$
$$\alpha\hat{h}_{i-1} + \hat{h} + \alpha\hat{h}_{i+1} = \sum_{j=1}^{5} \frac{b_j}{2}(h_{i+j} + h_{i-j}) \tag{4d}$$

$$i \in \{6, 7, \ldots, n-5\}$$
$$\alpha\hat{h}_{i-1} + \hat{h} + \alpha\hat{h}_{i+1} = \sum_{j=1}^{5} \frac{a_j}{2}(h_{i+j} + h_{i-j}) \tag{4e}$$

where $\alpha = 0.49$ ($0.3 \le \alpha \le 0.5$) and the a_j, b_j, $a_{j,i}$ are given in Table 1. It should be noted that a 10th-order filter is applied at interior points for $i \in \{6, 7, \ldots, n-5\}$ and an eighth-order filter is applied near boundaries for $i \in \{2, \ldots, 5\}$ and $i \in \{n-4, \ldots, n-1\}$.

The designations, EM0, EM1, EM0/FM, and EM1/FM are used to denote the following combinations of EM and FM schemes: EM0 designates zeroth-order EM without FM, EM1 designates first-order

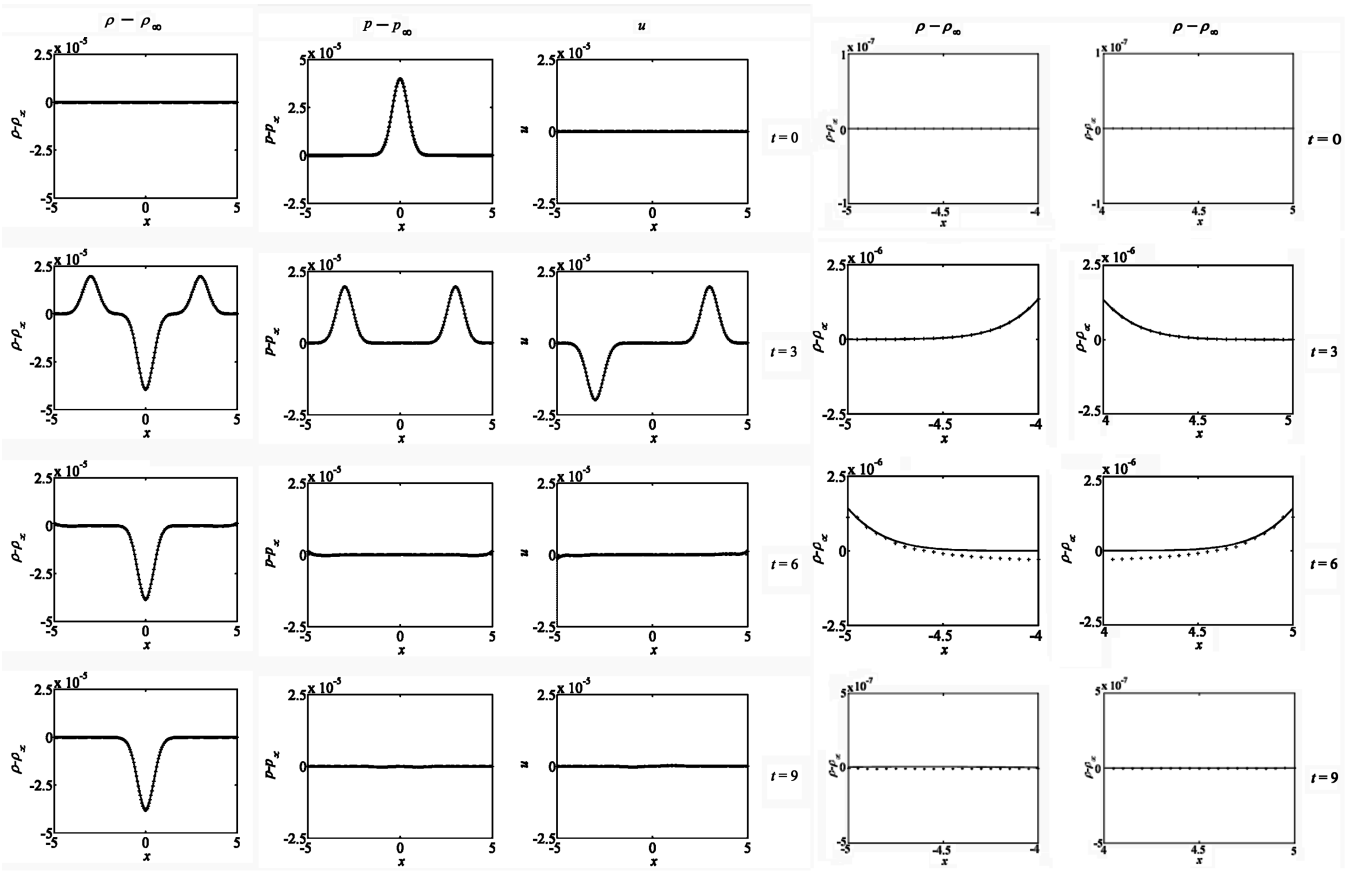

Fig. 2 a) The density, pressure, and velocity fluctuations along the x axis at four different t with zeroth-ordered extrapolation boundary conditions (with filter) EM0/FM: +, LBM; solid line, DNS. b) Enlarged snapshots of density fluctuation on left boundary, $x = [-5, -4]$ and on right boundary, $x = [4, 5]$ at $t = 0$, $t = 3$, $t = 6$, $t = 9$ with zeroth-ordered extrapolation boundary conditions (with filter) EM0/FM: +, LBM; solid line, DNS.

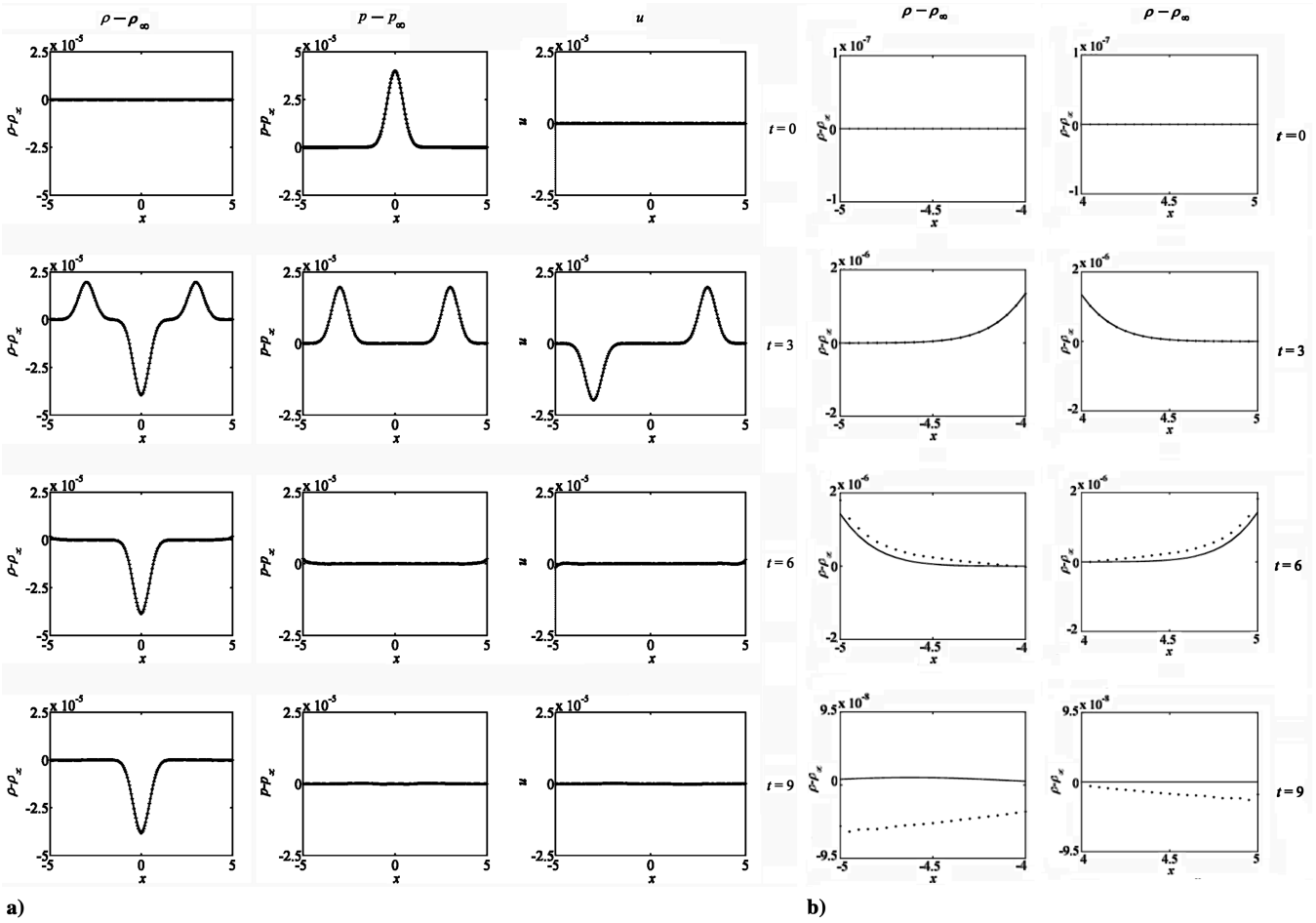

Fig. 3 a) The density, pressure, and velocity u fluctuations along the x axis at four different t with first-ordered extrapolation boundary conditions (with filter) EM1/FM: +, LBM; solid line, DNS. b) Enlarged snapshots of density fluctuation on left boundary, $x = [-5, -4]$ and on right boundary, $x = [4, 5]$ at $t = 0$, $t = 3$, $t = 6$, $t = 9$ with first-ordered extrapolation boundary conditions (with filter) EM1/FM: +, LBM; solid line, DNS.

EM without FM, EM0/FM designates zeroth-order EM with FM, and EM1/FM designates first-order EM with FM.

B. Type 2: C^1 Continuity

The basic idea of this method, hereafter designated as C^1 continuity, is to extrapolate whatever variables (f, first derivatives of f, etc.) chosen for consideration at the computational boundary based on at least two known points inside the domain. In addition, the inward f (or first derivatives of f) in all lattice directions is assumed to be zero. Lower-order extrapolation methods (e.g., zeroth and first order) are easy to adopt for finite-difference schemes up to third order. Generally, the order of accuracy of the method should be at most one order lower than that of the finite-difference scheme used for the numerical simulation. If not, the overall order of accuracy would be lowered [22]. No filter or buffer region is added to this scheme.

C. Type 3: ABC

An absorbing region is established based on the addition of dissipative and convective terms to the compressible Navier–Stokes equations in the case of DNS schemes. The prescribed flow (usually uniform mean flow) is achieved on the boundary by suppressing all undesirable disturbances within the region. Therefore no reflection is detected at the boundary. This can be seen by considering a prescribed flow with properties given by a flow with target properties. This concept can be extended to LBM where the absorption is implemented in the f equation which can be written in the buffer region for a 2-D problem as

$$\frac{\partial f}{\partial t} + \boldsymbol{\xi} \cdot \nabla f + \sigma(f^{\mathrm{eq}} - f_a) = -\frac{1}{\tau_{\mathrm{eff}}}(f - f^{\mathrm{eq}}) \tag{5}$$

where f_a has the same structure as the weighting factor A_i, $\sigma = \sigma_m(\delta/D)^2$, and σ_m is a constant to be specified. The target f_a is therefore achieved asymptotically towards the outer boundary of the absorbing region. This boundary scheme is referred to as ABC from this point on.

V. Results and Discussion

In the present study, an investigation into the performance of the three different nonreflecting boundary treatment schemes is carried out. The vehicles of this comparison are two classical aeroacoustic problems that have been investigated previously [26]. These two problems are as follows: case 1) propagation of a plane pressure pulse; case 2) propagation and interaction of an acoustic pulse with an entropy pulse and a vortex pulse. The benchmark solutions were provided by DNS calculations assuming a much larger computational domain. The DNS computational domain and the truncated domain for LBM simulations chosen for these two cases are specified in following sections. It is sufficient to note that in the DNS calculations, no filtering or damping is applied. In the first case, the initial size of the acoustic pulse L, c_∞, and mean density ρ_∞ are adopted as the reference quantities for normalization. The Reynolds number is defined as $Re = \rho_\infty c_\infty L/\mu_\infty$. In the second case, the initial size of the acoustic pulse L, uniform mean flow u_∞, and mean density ρ_∞ are adopted as the reference quantities for normalization. The Reynolds number and Mach number of the second case are defined as $Re = \rho_\infty u_\infty L/\mu_\infty$ and $M = u_\infty/c_\infty$. In both cases a

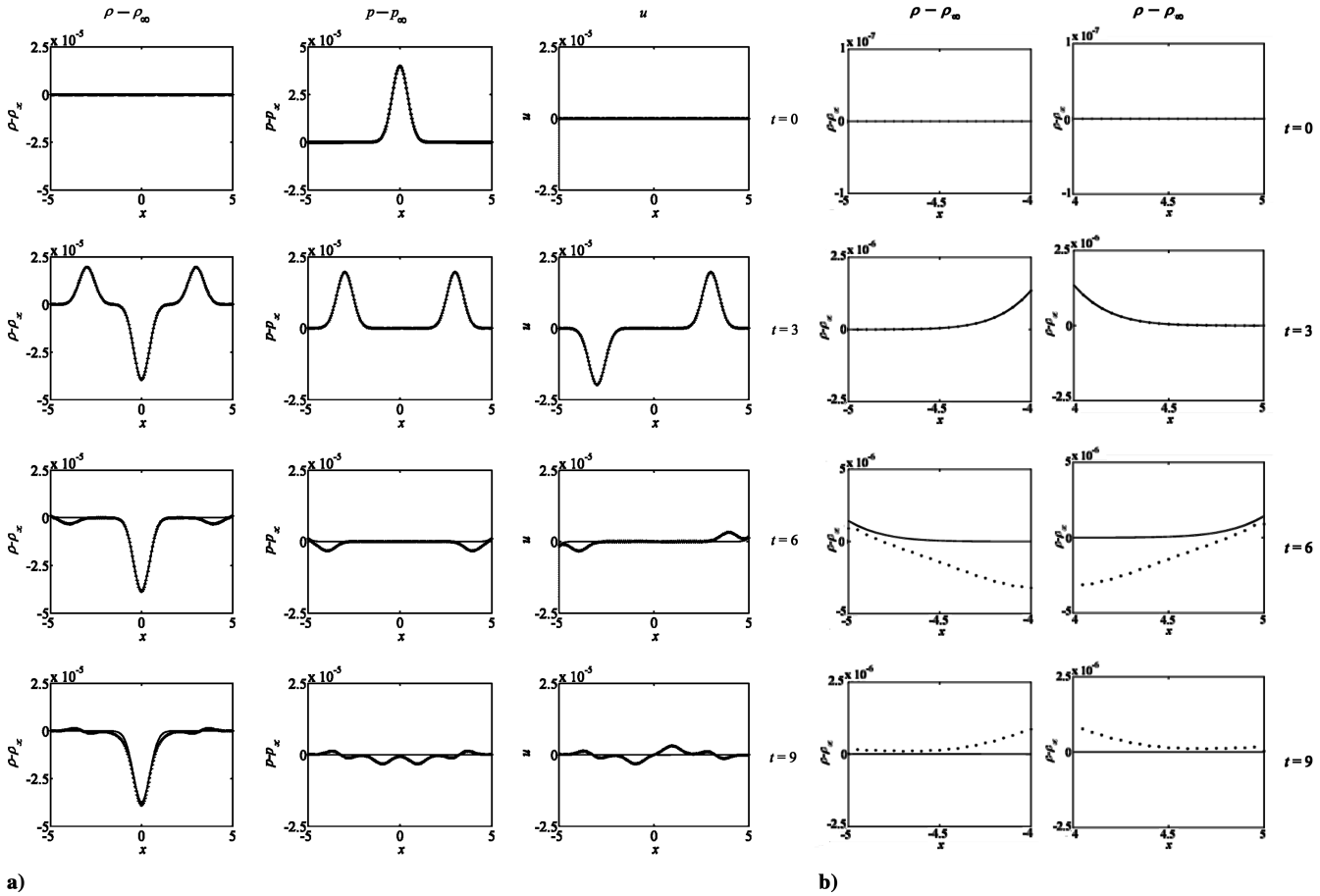

Fig. 4 a) The density, pressure, and velocity u fluctuations along the x axis at four different t with C^1 boundary conditions: +, LBM; solid line, DNS. b) Enlarged snapshots of density fluctuation on left boundary, $x = [-5, -4]$ and on right boundary, $x = [4, 5]$ at $t = 0, t = 3, t = 6, t = 9$ with C^1 boundary conditions: +, LBM; solid line, DNS.

uniform grid size of $\Delta x = \Delta y = 0.05$ and a time step of $\Delta t = 0.00001$ are used in all calculations for consistency of comparison. Here, x and y are the Cartesian coordinates with the propagation direction aligned with x, and μ_∞ is the reference fluid viscosity.

To demonstrate the validity and extent of the LBM simulations, the accuracy of the solutions are evaluated against the benchmark DNS solutions obtained using the larger domain with absorbing boundary treatment applied. The setup of absorbing boundary treatment applied to LBM is the same as that applied to DNS. A measure of the error between the LBM and DNS results of a macroscopic variable b is expressed in terms of the L_P integral norm

$$\|L_P(b)\| = \left[\frac{1}{M}\sum_{j=1}^{M}|b_{\mathrm{LBM},j} - b_{\mathrm{DNS},j}|^P\right]^{\frac{1}{P}} \tag{6}$$

for any integer p and its maximum

$$\|L_\infty(b)\| = \max_j |b_{\mathrm{LBM},j} - b_{\mathrm{DNS},j}| \tag{7}$$

Errors based on Eqs. (6) and (7) are calculated using the three NRBC outlined in the preceding sections. The error estimates for the pressure and velocity deduced from all three types of NRBC are tabulated in Tables 2–5.

A. Case 1: Propagation of a Plane Pressure Pulse

For this 1-D problem, the validity of those NRBC specified in Sec. III is tested by applying them on both the inlet and outlet boundary, while C^1 continuity is used on the top and bottom boundaries. As demonstrated in Li et al. [26], the large computational domain chosen for DNS simulation is $-10 \le x \le 10$ and $-1 \le y \le 1$, and the truncated size for LBM calculations is given by $-5 \le x \le 5$ and $-1 \le y \le 1$. This allows the present calculations to be compared with those presented using ZFG for boundary conditions [26]. In ABC, an absorbing region with a width of $D = 1$ is added to the inlet and outlet boundaries. Because $\Delta x = 0.05$, there are 20 grid points along the x direction in the absorbing region. No ABC is implemented at the top and bottom boundaries. The EM and C^1 continuity NRBC are applied to computational domains of the same size as ABC minus the absorbing region.

The initial conditions for the aerodynamic and acoustics fluctuations are specified as [35]

$$\rho = \rho_\infty, \qquad u = u_\infty, \qquad v = v_\infty, \qquad p = p_\infty + \varepsilon \exp(k) \tag{8}$$

where $k = -\ell_n\, 2 \times (x/0.08)^2$. For the plane pressure pulse problem considered here, $\rho_\infty = 1$, $u_\infty = 0$, $v_\infty = 0$, and $p_\infty = 1/\gamma$ are chosen as reference quantities, while $Re = 1000$ and $\varepsilon = 0.0001$ are specified. Using these reference quantities, the initial f^{eq} is specified according to Eqs. (2) and (3).

Calculations are carried out using the three types of boundary treatment schemes discussed in Sec. III. Four different combinations of the EM type are tested; they are the zeroth- and first-order EM with and without the use of filtering. Altogether, six different boundary conditions are investigated; they are EM0, EM0/FM, EM1, EM1/FM, C^1 continuity, and ABC. Although the EM boundary conditions work well for aerodynamic flow calculations [30–34], their suitability for one-step aeroacoustic simulations needs demonstration. These combinations of EM and FM could clearly demonstrate the necessity of having to implement FM in any one-step aeroacoustic simulations using EM and the relative merits of a zeroth- or first-order extrapolation.

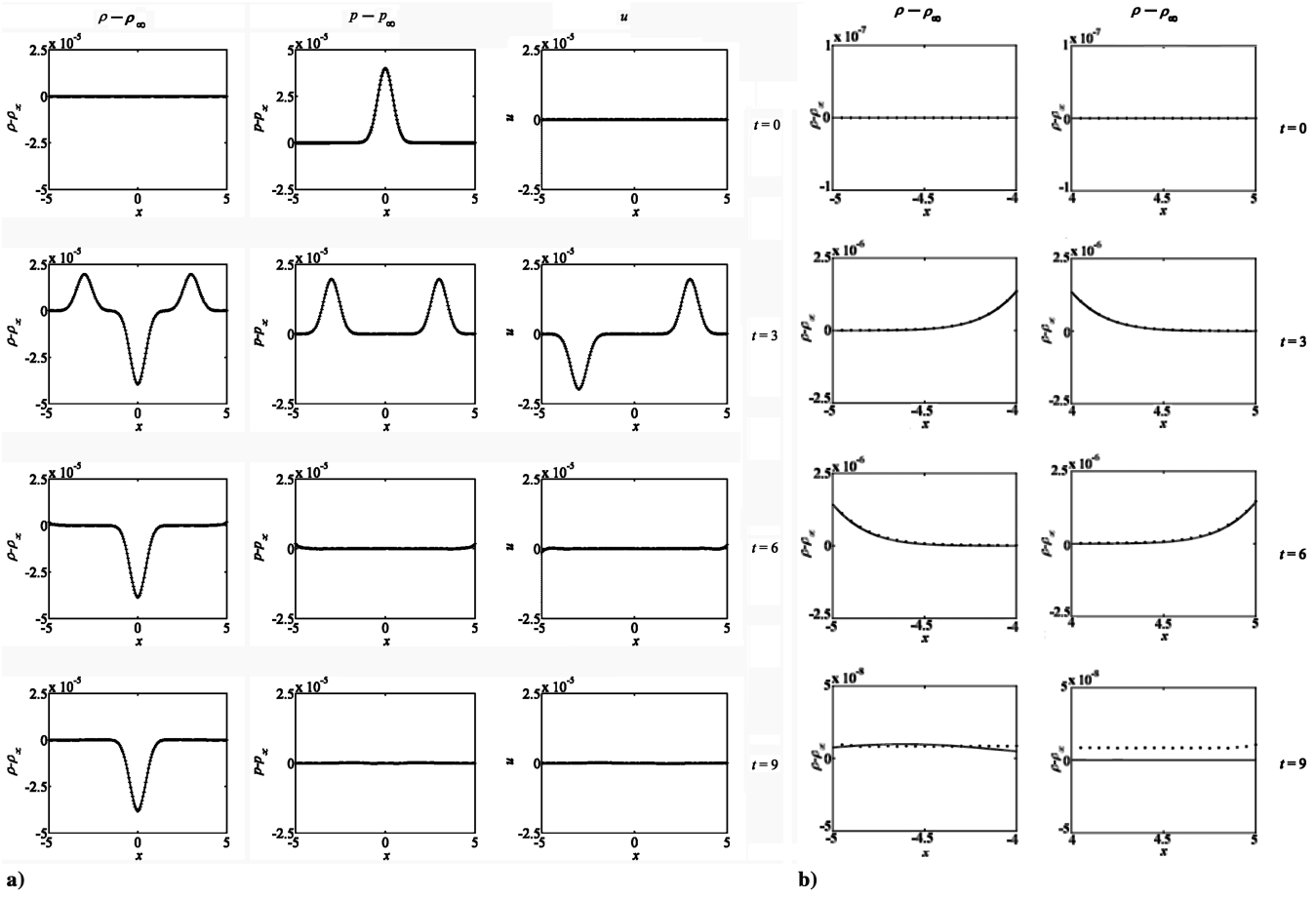

Fig. 5 a) The density, pressure and velocity u fluctuations along the x axis at four different t with absorbing boundary conditions: +, LBM; solid line, DNS. b) Enlarged snapshots of density fluctuation on left boundary, $x = [-5, -4]$ and on right boundary, $x = [4, 5]$ at $t = 0$, $t = 3$, $t = 6$, $t = 9$ with absorbing boundary conditions: +, LBM; solid line, DNS.

Absolute integral norm error $\|L_1(p)\|$, integral root mean square (rms) error norm $\|L_2(p)\|$, and the maximum error norm $\|L_\infty(p)\|$ are calculated at $t = 9$. Norm errors for fluctuating pressure p and the streamwise velocity u are determined using Eqs. (6) and (7) and the results for EM0, EM0/FM, EM1, EM1/FM, C^1 continuity, and ABC are tabulated in Tables 2 and 3. Among the nonreflecting boundary treatment schemes tested, three schemes give the best performance for the calculations of p and u. They are EM0/FM, EM1/FM, and ABC. Besides, ABC gives the least L_2 error among the three best performed nonreflecting boundary treatment schemes, with the same order of magnitude as previous calculations of the same pulse at $Re = 5000$ [26]. The worst performers are EM0 and EM1. This shows that filtering is necessary for one-step aeroacoustic simulation problems if these norm errors are to be reduced to minimum. Once filtering is applied, the difference between a zeroth-order extrapolation and a first-order one is negligibly small. This is the reason why EM0/FM and EM1/FM have essentially the same performance.

The plots of $(\rho - \rho_\infty)$, $(p - p_\infty)$, and u at $t = 0$, $t = 3$, $t = 6$, and $t = 9$ for the four NRBC schemes, EM0/FM, EM1/FM, C^1 continuity, and ABC, are shown in Figs. 2a, 3a, 4a, and 5a, respectively. From the EM0 and EM1 calculations, it is obvious that at $t = 9$ the waves are reflected back from the inlet and outlet boundaries. Therefore, these results are not shown. To depict the wave behavior more clearly at the inlet and outlet boundaries, blowups of the density at these locations are given in Figs. 2b, 3b, 4b, and 5b. It is clear that the errors at these boundaries are at least one order of magnitude less.

For the C^1 continuity scheme, even though the inward first derivatives of f at the boundaries are set to zero, disturbance waves are clearly visible as early as $t = 6$ (Fig. 4a). As a result, numerical results deduced from these three schemes are not in agreement with the reference DNS solution and the clean exit of all waves at $t = 9$ shown in the DNS result is not replicated correctly by the three boundary treatment schemes. The calculated results given by EM0/FM, EM1/FM, and ABC (Figs. 2, 3, and 5) are in excellent agreement with the DNS result and they show a clean exit of all waves at $t = 9$.

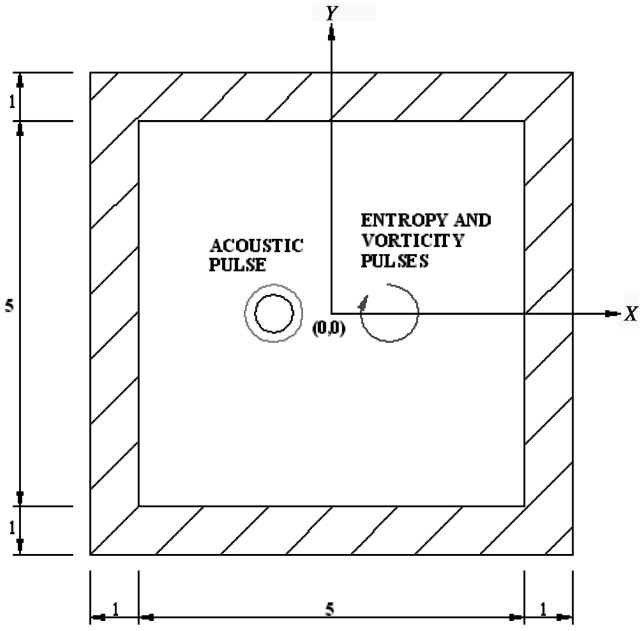

Fig. 6 The acoustic, entropy, and vorticity pulse propagation in a uniform stream configuration for case 2 (hatched area as buffer region).

These results further support the conclusion drawn from a comparison of the error norm in Tables 2 and 3. Because a 10th-order filtering scheme [2,3] is used in the extrapolation method, the results therefore suggest that reflections from the inlet and outlet boundary are mainly due to high-frequency components in the computational domain. This explains why extrapolation method can be applied to low-order LBM schemes [30–34], because high-frequency disturbances are not being resolved by these low-order LBM schemes. The ABC, on the other hand, is equally applicable for low- as well as high-order LBM schemes; therefore, it can be used effectively for the calculations of aerodynamic flow alone as well as for one-step aeroacoustics problems. Because ZFG has already been validated as a viable nonreflecting boundary condition for this problem [26], up to this point, three different types of nonreflecting boundary treatment schemes (EM0/FM and EM1/FM can be considered as the same type) have been proven appropriate. Of these, ABC is an extension of a current scheme used in DNS to LBM.

B. Case 2: Propagation of Acoustic, Entropy, and Vortex Pulses

As before, the large computational domain is specified as $-10 \leq x \leq 10$ and $-10 \leq y \leq 10$, and the acoustic pulse is initialized at $x = -1$ and $y = 0$, whereas the entropy pulse and the vorticity pulse are initialized at $x = 1$ and $y = 0$. The truncated computational domain for EM1/FM is given by $-2.5 \leq x \leq 2.5$ and $-2.5 \leq y \leq 2.5$. In the case of the ABC, an absorbing region with $D = 1$ is specified on all boundaries. Consequently, the computational domain for the ABC boundary treatment is $-3.5 \leq x \leq 3.5$ and $-3.5 \leq y \leq 3.5$. The initial conditions for the aerodynamic and acoustics fluctuations are specified as

$$\rho = \rho_\infty + \varepsilon_1 e^a + \varepsilon_2 e^b, \qquad u = u_\infty + \varepsilon_2 e^b$$
$$v = v_\infty - \varepsilon_2 (x-1) e^b, \qquad p = p_\infty + \varepsilon_1 e^a / M^2 \tag{9a}$$

$$a = -\ell_n 2 \left(\frac{(x+1)^2 + y^2}{0.2^2} \right) \tag{9b}$$

$$b = -\ell_n 2 \left(\frac{(x-1)^2 + y^2}{0.4^2} \right) \tag{9c}$$

where $\varepsilon_1 = 0.0001$, $\varepsilon_2 = 0.001$. For this problem, the reference quantities are specified as $\rho_\infty = 1$, $u_\infty = 1$, $v_\infty = 0$, and $p_\infty = 1/\gamma M^2$, while $Re = 1000$ and $M = 0.2$ are chosen, which are the same as those previously reported [35]. Using these reference quantities, the initial f^{eq} is specified according to Eqs. (2) and (3). The problem setup is visualized in Fig. 6.

This problem has also been treated in Li et al. [26], and good agreement with DNS results is obtained using the ZFG boundary treatment scheme. In the preceding example, it has been shown that among the three types of boundary treatment schemes considered, only EM/FM and ABC can reproduce the DNS results in a truncated computational domain. Even then, all six schemes are used to perform the LBM calculations of this problem and the calculated error norms are tabulated in Tables 4 and 5 for comparison. Again, $\|L_1(p)\|$, $\|L_2(p)\|$, and $\|L_\infty(p)\|$ at $t = 2.6$ for EM0, EM0/FM, EM1, EM1/FM, C^1 continuity, and ABC are calculated and shown in Tables 4 and 5. Only the norm errors of p and u are determined. As expected, EM0/FM, EM1/FM, and ABC yield the least errors, whereas the C^1 continuity scheme gives errors that are in between those of EM0 and EM1, and EM0/FM, EM1/FM, and ABC. The worst performers are EM0 and EM1. Again, ABC gives the least L_1, L_2, and L_∞ error among all schemes tested.

A sample comparison of the LBM calculations invoking ABC with those of DNS for case 2 is shown in Fig. 7. The panels under 7a are pressure plots, whereas those under 7b are velocity contours. Altogether four different times are shown ranging from $t = 0.1$ to $t = 2.6$. The solution in the upper part of each panel is due to LBM and the lower part is the corresponding DNS simulation obtained

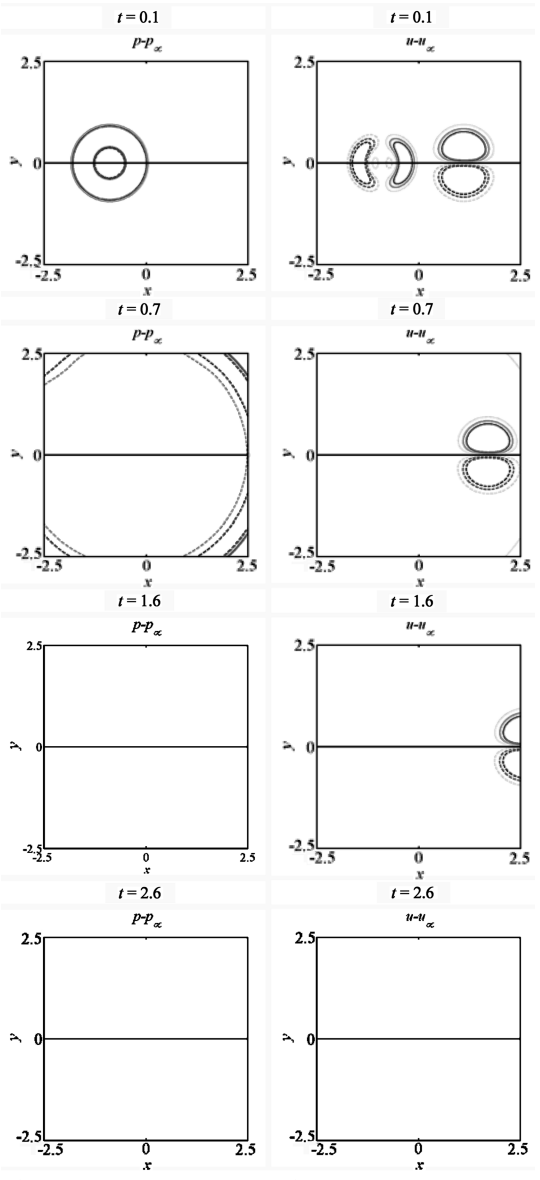

Fig. 7 Comparison of LBM solutions using ABC (upper half) with DNS solutions (lower half): a) pressure fluctuation (six contours equally distributed between -5×10^{-5} and 5×10^{-5}); b) streamwise velocity fluctuation (six contours equally distributed between -6×10^{-5} and 6×10^{-5}).

using a larger computational domain. It can be seen that by $t = 2.6$, the pulses have completely exited the computational domain defined by $-2.5 \leq x \leq 2.5$ and $-2.5 \leq y \leq 2.5$; that is, the actual domain not counting the absorbing region assumed for the LBM simulation. The solutions obtained using both LBM and DNS are very clean and there is essentially no reflection of waves at the boundaries. It should be pointed out that the computational domain for the LBM is only $-3.5 \leq x \leq 3.5$ and $-3.5 \leq y \leq 3.5$ compared to a domain of $-10 \leq x \leq 10$ and $-10 \leq y \leq 10$ for the DNS. This shows that LBM with ABC is a viable alternative to DNS with buffer region for direct aeroacoustic simulations.

VI. Conclusions

There are three objectives to this study. The first is to determine what commonly used NRBC for DNS simulations could be extended to LBM. The second is to ascertain whether the same accuracy could be achieved using a truncated computational domain compared to that required by DNS. The third is to identify best-performing NRBC for one-step LBM simulation of aeroacoustic problems. This

investigation gives rise to three different types of NRBC schemes that could be extended to LBM and they are the filtering (FM) type, the C^1 continuity type, and the absorbing (ABC) type. In addition, two other NRBC schemes that have been used previously for LBM simulations have been extended to one-step LBM aeroacoustic calculations. These are the extrapolation (EM) type and the zero f gradient (ZFG) type. The FM type and the EM type are tested in a mixed manner. Because the ZFG has already been proven to be valid for one-step LBM in [26], the present investigation does not include it in the final assessment.

Two aeroacoustic problems, namely, the propagation of a plane pressure pulse and the propagation of an acoustic pulse, an entropy pulse, and a vorticity pulse in a mean flow, are used as vehicles to test the different NRBC schemes. Altogether, six different schemes are tested; they are EM0, EM0/FM, EM1, EM1/FM, C^1 continuity, and ABC. Of these six, only EM0/FM, EM1/FM, and ABC are capable of yielding results that are essentially identical to those deduced from a one-step DNS simulation using a much larger computational domain with no boundary treatment. Overall, ABC performs the best. This result together with the previous study using ZFG gives four appropriate and applicable NRBC for one-step LBM simulation of aeroacoustic problems.

Acknowledgment

Support from the Research Grants Council of the Government of the Hong Kong Special Administrative Region given under Grant Nos. PolyU5174/02E, PolyU5303/03E, and PolyU1/02C is gratefully acknowledged.

References

[1] Lele, S. K., "Compact Finite Schemes with Spectral-Like Resolution," *Journal of Computational Physics*, Vol. 103, No. 1, 1992, pp. 16–42.

[2] Gaitonde, D. V. and Visbal, M. R., "Further Development of a Navier-Stokes Solution Procedure Based on Higher-Order Formulas," AIAA Paper 99-C0557, 1999.

[3] Visbal, M. R., and Gaitonde, D. V., "Very High-Order Spatially Implicit Schemes for Computational Acoustics on Curvilinear Meshes," *Journal of Computational Acoustics*, Vol. 9, No. 4, 2001, pp. 1259–1286.

[4] Leung, R. C. K., Li, X. M., and So, R. M. C. "Comparative Study of Nonreflecting Boundary Condition for One-Step Duct Aeroacoustic Simulation," *AIAA Journal*, Vol. 44, No. 3, 2006, pp. 664–667.

[5] Frisch, U., d'Humières, D., Hasslacher, B., Lallemand, P., Pomeau, Y., and Rivet, J.-P., and Pomeau, Y., "Lattice Gas Hydrodynamics in Two and Three Dimensions," *Complex Systems*, Vol. 1, No. 4, 1987, pp. 649–707.

[6] Lallemand, P., and Luo, L.-S., "Theory of the Lattice Boltzmann Method: Dispersion, Dissipation, Isotropy, Galilean Invariance, and Stability," *Physical Review E (Statistical Physics, Plasmas, Fluids, and Related Interdisciplinary Topics)*, Vol. 61, No. 6, 2000, pp. 6546–6562.

[7] Lallemand, P., and Luo, L.-S., "Theory of the Lattice Boltzmann Method: Acoustic and Thermal Properties in Two and Three Dimensions," *Physical Review E (Statistical Physics, Plasmas, Fluids, and Related Interdisciplinary Topics)*, Vol. 68, Sept. 2003, p. 036706.

[8] Ricot, D., Maillard, V., and Bailly, C., "Numerical Simulation of Unsteady Cavity Flow Using Lattice Boltzmann Method," AIAA Paper 2002-2532, 2002.

[9] Tsutahara, M., Kataoka, T., Takada, N., Kang, H.-K., and Kurita, M., "Simulations of Compressible Flows by Using the Lattice Boltzmann and the Finite Difference Lattice Boltzmann Methods," *Computational Fluid Dynamics Journal*, Vol. 11, No. 1, 2002, pp. 486–493.

[10] Kang, H.-K., Ro, K.-D., Tsutahara, M., and Lee, Y.-H., "Numerical Prediction of Acoustic Sounds Occurring by the Flow around a Circular Cylinder," *KSME International Journal*, Vol. 17, No. 8, 2003, pp. 1219–1225.

[11] Wilde, A., "Calculation of Sound Generation and Radiation from Instationary Flows," *Computers and Fluids*, Vol. 35, Nos. 8–9, 2006, pp. 986–993.

[12] Mallick, S., Shock, R., and Yakhot, V., "Numerical Simulation of the Excitation of a Helmholtz Resonator by a Grazing Flow," *Journal of the Acoustical Society of America*, Vol. 114, No. 4, 2003, pp. 1833–1840.

[13] Danforth, A. L., and Long, L. N., "Nonlinear Acoustic Simulations Using Direct Simulation Monte Carlo," *Journal of the Acoustical Society of America*, Vol. 116, No. 4, 2004, pp. 1948–1955.

[14] Philippi, P. C., Hegele, L. A., dos Santos, L. O. E., and Surmas, R., "From the Continuous to the Lattice Boltzmann Equation: The Discretization Problem and Thermal Models," *Physical Review E (Statistical Physics, Plasmas, Fluids, and Related Interdisciplinary Topics)*, Vol. 73, May 2006, p. 056702.

[15] Roe, P. L., "Characteristic-Based Schemes for the Euler Equations," *Annual Review of Fluid Mechanics*, Vol. 18, 1986, pp. 337–365.

[16] Giles, M. B., "Nonreflecting Boundary Conditions for Euler Equation Calculations," *AIAA Journal*, Vol. 28, No. 12, 1990, pp. 2050–2058.

[17] Poinsot, T. J., and Lele, S. K., "Boundary Conditions for Direct Simulations of Compressible Viscous Flows," *Journal of Computational Physics*, Vol. 101, No. 1, 1992, pp. 104–129.

[18] Colonius, T., Lele, S. K., and Moin, P., "Boundary Conditions for Direct Computation of Aerodynamic Sound Generation," *AIAA Journal*, Vol. 31, No. 9, 1993, pp. 1574–1582.

[19] Kim, J. W., and Lee, D. J., "Generalized Characteristic Boundary Conditions for Computational Aeroacoustics," *AIAA Journal*, Vol. 38, No. 11, 2000, pp. 2040–2049.

[20] Engquist, B., and Majda, A., "Absorbing Boundary Conditions for the Numerical Simulation of Waves," *Mathematics of Computation*, Vol. 31, July 1977, pp. 629–651.

[21] Ta'asan, S., and Nark, D. M., "An Absorbing Buffer Zone Technique for Acoustic Wave Propagation," AIAA Paper 95-0146, 1995.

[22] Freund, J. B., "Proposed Inflow/Outflow Boundary Condition for Direct Computation of Aerodynamic Sound," *AIAA Journal*, Vol. 35, No. 4, 1997, pp. 740–742.

[23] Hu, F. Q., "A Stable, Perfectly Matched Layer for Linearized Euler Equations in Unsplit Physical Variables," *Journal of Computational Physics*, Vol. 173, No. 2, 2001, pp. 455–480.

[24] Loh, C. Y., "On a Non-Reflecting Boundary Condition for Hyperbolic Conservation Laws," AIAA Paper 2003-3975, 2003.

[25] Loh, C. Y., and Jorgenson, P. C. E., "A Robust Absorbing Boundary Condition for Compressible Flows," AIAA Paper 2005-4716, 2005.

[26] Li, X. M., Leung, R. C. K., and So, R. M. C., "One-Step Aero-Acoustics Simulation Using Lattice Boltzmann Method," *AIAA Journal*, Vol. 44, No. 1, 2006, pp. 78–89.

[27] Li, X. M., So, R. M. C., and Leung, R. C. K., "Propagation Speed, Internal Energy and Direct Aeroacoustic Simulation Using LBM," *AIAA Journal*, Vol. 44, No. 12, 2006, pp. 2896–2903.

[28] Bhatnagar, P., Gross, E. P., and Krook, M. K., "A Model for Collision Processes in Gases, 1. Small Amplitude Processes in Charged and Neutral One-Component Systems," *Physical Review*, Vol. 94, No. 3, 1954, pp. 515–525.

[29] Li, X. M., "Computational Aeroacoustics Using Lattice Boltzmann Method," Ph.D. Thesis, Dept. of Mechanical Engineering, Hong Kong Polytechnic University, Hong Kong, 2006.

[30] Chen, S., Martinez, D., and Mei, R., "On Boundary Conditions in Lattice Boltzmann Methods," *Physics of Fluids*, Vol. 8, No. 9, 1996, pp. 2527–2536.

[31] Maier, R., Bernard, R. S., and Grunau, D. W., "Boundary Conditions for the Lattice Boltzmann Method," *Physics of Fluids*, Vol. 8, No. 7, 1996, pp. 1788–1801.

[32] Guo, Z., and Zhao, T. S., "Explicit Finite-Difference Lattice Boltzmann Method for Curvilinear Coodinates," *Physical Review E (Statistical Physics, Plasmas, Fluids, and Related Interdisciplinary Topics)*, Vol. 67, No. 6, 2003, pp. 1–12.

[33] Yu, D., Mei, R., and Shyy, W., "Improved Treatment of the Open Boundary in the Method of Lattice Boltzmann Equation: General Description of the Method," *Progress in Computational Fluid Dynamics*, Vol. 5, Nos. 1–2, 2005, pp. 3–12.

[34] Bennett, A. F., Taylor, J. R., and Chua, B. S., "Lattice Boltzmann Open Boundaries for Hydrodynamic Models," *Journal of Computational Physics*, Vol. 203, No. 1, 2005, pp. 89–111.

[35] Tam, C. K. W., and Webb, J. C., "Dispersion-Relation-Preserving Finite Difference Schemes for Computational Acoustics," *Journal of Computational Physics*, Vol. 107, No. 2, 1993, pp. 262–281.

X. Zhong
Associate Editor